Methyl group rotation in trimethylaluminium

2002 J. Phys.: Condens. Matter 14 1833

(http://iopscience.iop.org/0953-8984/14/8/312)

INSTITUTE OF PHYSICS PUBLISHING JOURNAL OF PHYSICS: CONDENSED MATTER

J. Phys.: Condens. Matter **14** (2002) 1833–1845 PII: S0953-8984(02)30373-4

Methyl group rotation in trimethylaluminium

M Prager[1], H Grimm[1], S F Parker[2], R Lechner[3], A Desmedt[3], S McGrady[4] and E Koglin[5]

[1] Institut für Festkörperforschung, Forschungzzentrum Jülich, D-52425 Jülich, Germany
[2] ISIS Facility, Rutherford-Appleton Laboratory, Chilton, Didcot, Oxon OX11 0QX, UK
[3] Hahn-Meitner Institut, Glienickershrasse 100, D-14109 Berlin, Germany
[4] Department of Chemistry, Kings College, Strand, London WC2R 2LS, UK
[5] Institut für Angewandte Physikalische Chemie, Forschungzzentrum Jülich, D-52425 Jülich, Germany

Received 25 October 2001
Published 15 February 2002
Online at stacks.iop.org/JPhysCM/14/1833

Abstract

The stable molecular unit of trimethylaluminium is the dimer linked via bridging methyl groups. Neutron spectroscopy is used to determine internal and external modes from μeV (rotational tunnelling transitions of methyl groups, stochastic rotational jumps) to meV (deformations, librations, phonons etc). The dimer appears to be non-rigid with a very soft bend mode about an axis connecting the two bridging methyl groups. Rotational potentials are derived from tunnelling modes and barrier heights deduced from quasielastic spectra. Internal modes obtained from *ab initio* calculations for the isolated dimer are consistent with measured vibrations with respect to eigenenergies and band intensities calculated by the CLIMAX program. The bridging CH_3 group shows the strongest and almost purely intramolecular potential due to a loss of a single bond axis of its pentacoordinated carbon atom.

(Some figures in this article are in colour only in the electronic version)

1. Introduction

The overwhelming majority of studies of methyl rotational dynamics [1] are performed on organic molecules. These materials offer the same rather well defined chemical bond of the methyl group within a given class of compounds, e.g. aromatic rings, but methyl groups are found in a large variety of molecules and environments. Organometallic compounds on the other hand allow one to vary the bond strength systematically within a homologous series of compounds by varying the metal ion. The increasing instability of tetramethyl metal compounds with increasing mass/size of the central metal ion is a typical example. While neopentane at the beginning of the series can be safely handled, tetramethyl-lead at its end is self-explosive. The decreasing strength of the rotational potentials of the methyl groups systematically reflects these properties [2].

The group III trimethyl compounds form a similar class. Due to their thermal instability the materials can be used for doping semiconductors with Al, Ga, In and Tl by decomposing the gaseous material at the surface of a hot substrate. There is an extended literature on the best system to use for clean chemical vapour deposition [3]. Aluminium alkyls are further used as Ziegler–Natta catalysts in polymerization of olefins [4]. The properties exploited are related to the fact that the molecule is electrically not saturated. For this reason trimethyl aluminium forms *dimers* $Al_2(CH_3)_6$ with each Al atom approximately tetrahedrally surrounded by methyl groups. The two tetrahedra are linked via one edge. This configuration is already found in the gas phase [5] and for matrix-isolated molecules [6]. The dimer is also the building unit in the crystalline state. The most interesting question concerns the structure around the unique bridging methyl group. Various single-crystal structure studies have been undertaken using x-rays [7–9]. At $T = -50\,^{\circ}\mathrm{C}$ it is shown that the space group of $Al(CH_3)_3$ is $C2/c$ and that dimers $Al_2(CH_3)_6$ are the molecular building units. The skeletal structure of the molecule shows high symmetry: the aluminium atoms and the bridging carbons lie in a plane. The centre of gravity of the dimer is an inversion centre [9] and yields three inequivalent types of methyl group. The dimerization is connected with a coordination number 4 of the aluminium which exceeds its number of free valences (three) and leads to electron deficiency in the Al–C bond of the two bridging methyl groups. The reduced electron density is accompanied by a $\sim$10% increase of the bond length. For a long time it was unclear whether the bridging methyl group is symmetrically arranged between the two monomers or whether there is a side with a carbon and a side with a hydrogen bond. Even the most recent x-ray diffraction work [9] leaves some doubts due to difficulty of precisely locating protons.

A recent neutron diffraction [10] study has located the hydrogen atoms. The space group is found to be $C2/c$ with two dimers in the unit cell down to a temperature of $T = 4.5$ K. Including the proton positions, there is still a centre of inversion linking the two halves of the dimer. Bridging methyl groups are symmetric and do not involve hydrogen bonding.

NMR T_1-measurements have found an average barrier to rotation for methyl groups of only about 3.5 kJ mol^{-1} [11]. For a threefold cosine potential the corresponding tunnel splitting of the librational ground state is 2 μeV. The problem with this work is that its data analysis has neglected the presence of inequivalent methyl groups.

According to infrared spectra, the methyl groups rotate almost freely if matrix isolated in an argon lattice [6].

$Al(CH_3)_3$ represents a model electron deficiency compound. The electron deficiency leads to changes of the coordination number of Al in the dimer and significant deviations from standard bond lengths. Because of these fundamental properties, the molecule has attracted theoretical interest recently. The power of modern computers is just high enough to allow calculation of minimum-energy configurations with *ab initio* techniques for molecules of this size. The soft internal degrees of freedom on the other hand represent an extraordinary challenge to the accuracy of the computer code. There are two papers available which analyse the configuration of dimers, eigenmode energies and rotational barriers with the GAUSSIAN94 program [4, 17]. Both papers obtained a stable ground state. Unlike the experimentally determined structure in the solid phase [7–10], the isolated dimer shows lower symmetry in both calculations. If one Al atom and the two bridging carbon C_b atoms define a plane, the second Al atom is moved out of this plane by 3.3° (figure 5). The eclipsed configuration of the bridging methyl groups is maintained [9, 10]. The planes of terminal carbons C_t and the corresponding aluminium are parallel in both cases. In [17] the rotational barrier of bridging CH_3 is estimated to be 20 kcal mol^{-1}. The practical aim is to optimize its catalytic properties by suitable substitutions, e.g. chlorination [4].

It is the aim of this paper to shed light on this interesting system by using spectroscopic techniques. Incoherent inelastic neutron scattering is especially well suited for studying a solid mainly consisting of protons. An energy range $0.001 \leqslant \Delta E$ (meV) $\leqslant 500$ covers all excitations from tunnelling to internal modes.

High-resolution spectroscopy can reveal rotational dynamics giving quantitative access to methyl rotational potentials. The tunnelling spectra measured around He temperature will allow us to determine precisely the number of inequivalent methyl groups, their occurrence probabilities and the rotational potentials of the groups whose tunnel splittings can be resolved [1]. By combining tunnel splittings with librational excitations measured in the meV regime directly and assigned to a tunnel splitting by the temperature dependence of the broadening of a tunnelling line [12] or with barrier height obtained from temperature-dependent quasielastic spectra, a refinement of the shape of the rotational potential becomes possible.

Low-resolution spectroscopy in a wide energy band will yield lattice and internal modes and will allow their assignment by an eigenmode analysis. The intermolecular interaction will be modelled by force fields. Internal eigenmodes are characteristic of the building units of the crystal, allowing one to distinguish between monomers and dimers.

The results obtained from neutron spectroscopy will be compared with *ab initio* calculations of the characteristic molecular unit, the dimer, using the GAUSSIAN98 program system [13]. This will give a basis for testing the interpretation of the experimental data, on one hand, but also the reliability of an *ab initio* method for a delicately balanced system.

2. Experiment and results

2.1. Sample preparation

The protonated material is a commercial product. For the use in semiconductor technology the material must be sufficiently pure that it can be used without any further treatment. The colourless liquid was distilled in a vacuum line into a stainless steel cell of 0.5 mm thickness and lateral dimensions (35×40) mm^2.

The deuterated material was prepared by the reaction of $(CD_3)_2Hg$ with Al using an adaptation of a literature procedure [10, 14]. The product was purified by fractional condensation in vacuo. For further use the material was finally sealed into a glass capillary of 8 mm diameter and a height of 30 mm.

2.2. Rotational tunnelling

The protonated material was investigated by high-resolution spectroscopy. The flat stainless steel sample holder contained a 0.5 mm thick sample and was mounted at an angle of 45° to the neutron beam. The calculated scattering probability is 27%.

The backscattering spectrometer at the FRJ2-DIDO reactor at the research centre Jülich, Germany, was used in the offset configuration to study the tunnelling spectra. An energy regime $-32 < \hbar\omega$ (μeV) < 3 was accessible with an energy resolution of $\delta E \sim 1.5$ μeV. Spectra taken at various temperatures in the range $4.1 < T$ (K) < 28.9 are shown in figure 1. The energy resolution and the detector efficiencies were determined by a vanadium run. A constant background was taken into account. The scattering function consists of an elastic δ-function and three Lorentzians for two resolved tunnel transitions and the related quasielastic components [15]. This theoretical spectrum was convoluted with the measured resolution function (vanadium run). Since the tunnelling lines soon overlap with increasing temperature, the intensity ratio 1:1 of the two transitions, determined at the lowest temperature,

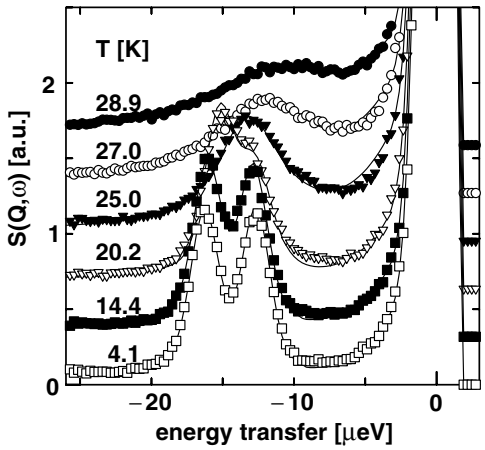

Figure 1. Temperature-dependent tunnelling spectra of $Al_2(CH_3)_6$. Instrument: BSS, FZJ Jülich. Average momentum transfer: $Q = 1.64$ Å. Solid curves are fits (see the text).

Table 1. The temperature dependence of the tunnelling frequencies and linewidths. From the Arrhenius law, the related activation energies $E_{S/W}$ (S = shift, W = width) are derived.

Temperature (K)	$\hbar\omega_1$ (μeV)	Γ_1 (μeV)	$\hbar\omega_2$ (μeV)	Γ_2 (μeV)	I_{inel}/I_{el} ($Q = 1.34$ Å^{-1})
4.1	12.63	0.15	16.24	0.18	0.093
14.4	12.81	0.19	16.04	0.16	Fixed
20.2	12.75	0.64	15.23	0.19	Fixed
25.0	13.36	1.47	12.27	3.06	Fixed
27.0	12.88	3.3	11.14	3.3	Fixed
28.9	11.48	4.1	9.99	6.8	Fixed
$E_{S/W}$ (meV)	—	12.0	10.3	—	

was fixed for all temperatures. This reduces the number of free parameters and stabilizes the fit by avoiding correlations. The quasielastic component in the tunnel spectrum was attributed to the intensity sum of the two tunnelling lines. Its width was fixed to that of the tunnelling line at the highest energy transfer. Transition energies, linewidths and the ratio of inelastic and elastic intensities obtained at the temperatures investigated are shown in table 1.

A test run performed on IN5 of the ILL showed no further tunnelling line up to the energy of the free rotor.

The scattering function of a tunnelling methyl group with its elastic and inelastic structure factors is well known [15]. On this basis, the ratio of inelastic and elastic intensity can be calculated for any combination of resolved and unresolved or out-of-range tunnelling rotors. On the basis of the neutron diffraction experiment [10] we assume that tunnelling of two thirds of the methyl groups is resolved while the remaining third scatter purely elastically. The scattering function normalized to the scattering of one proton is then

$$S(Q,\omega) = \sum_i (5 + 4j_0(Qd))\delta(\omega) + (2 - 2j_0(Qd))\delta(\omega - \omega_{ti}) + \delta(\omega + \omega_{ti}) \tag{1}$$

and the relation of the intensity of one tunnelling transition to the complete elastic intensity is in our case ($n = 3$, 2 resolved lines)

$$\frac{I_{inel}}{I_{el}} = \frac{2 - 2j_0(Qd)}{19 + 8j_0(Qd)}. \tag{2}$$

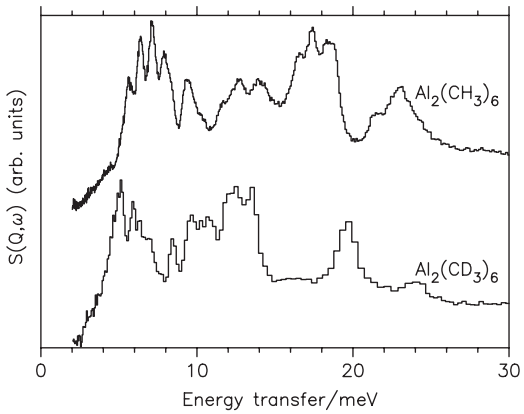

Figure 2. The low-energy regime of the neutron scattering spectra of $Al_2(CH_3/D_3)_6$. Instrument: TOSCA at the ISIS Facility, RAL, UK. Sample temperature: $T \sim 13$ K. Top: protonated material. Bottom: deuterated sample.

$j_0(Qd)$ is the spherical Bessel function with the proton–proton distance $d = 1.76$ Å and moment transfer Q. To test a structural model using its (elastic incoherent) structure factor, one has to choose a detector which is not contaminated by other elastic scattering. In our case the detector at 84° scattering angle shows the weakest elastic scattering. For its Q-value one calculates $I_{inel}/I_{el} = 0.063$ which is smaller than the experimental result of 0.093 (table 1). The increased inelastic intensity is most probably due to multiple scattering. Double scattering mainly transfers intensity from the strong elastic line to the tunnelling peaks. Given a scattering probability S, the double-scattering probability is of the order of S^2. For $S = 27\%$, S^2 is just of the right order to correct for the observed deviation from the theoretically expected ratio.

The exponential variation of the widths of the tunnelling lines with temperature follows Arrhenius laws and allows one in general to extract the librational energies of the corresponding methyl groups from its slope. The shift is related with a reduced activation energy [12]. Due to the overlap of the lines, the parameters are strongly correlated in trimethylaluminium and thus affected by significant errors. The energies obtained from the broadening in one case and the shift in the other are shown in table 1. Due to the clear theoretical background and the many experimental confirmations [1], these values help us to identify librational modes in the spectra taken on the inverse time-of-flight spectrometer TOSCA (see the next subsection).

2.3. Lattice and internal modes

The recently optimized TFXA spectrometer, now called TOSCA, at the ISIS Facility of the Rutherford Appleton Laboratory, UK, was used to measure the excitations in the energy regime 2–500 meV for the hydrogenated and deuterated compounds. The sample temperatures were lower than 15 K. Measuring times correspond to an integrated proton current of ∼2200 μA h. The spectra of protonated and deuterated materials are shown in figure 2. The small quantity of deuterated material available explains the lower quality of the corresponding data set. Assignments were done at first on the basis of isotopic shifts (especially for low-lying librational modes) and by comparison with the *ab initio* calculation (see below), and are shown in table 2.

Dimerization influences inelastic spectra in two ways. At first the number of internal modes increases from monomers to dimers. While molecular vibrations are characteristic of the building unit, eigenmodes of soft internal modes may be strongly influenced by

Table 2. The inelastic neutron scattering (INS) was measured in the solid state, the infrared (IR) in the gas phase. *Ab initio* calculations were performed for the isolated dimer.

Eigenenergies (cm^{-1})				
Hydrogenated (INS)	Deuterated (INS)	Hydrogenated (IR)	Hydrogenated (GAUSSIAN94)	Mode character
45	40			Acoustic phonons
51	46		57	Butterfly, whole molecule
58	48			Acoustic phonons
64	55			Acoustic phonons
76	69		136	Deformation, whole molecule
96	76		88/96	Torsion, $C_tH_3(2) + C_tH_3(2')$
101			92	Torsion, all C_tH_3
113	88		105/106	Torsion, $C_tH_3(2,2')$
134			152	Torsion, C_bH_3
141	99			Torsion, C_bH_3
149	111		152	Torsion, C_bH_3
174	160	175	168	Deformation, whole molecule
187	160		194	In-phase z-translation, C_bH_3
266	193		281	Anti-phase z-translation (shear), C_bH_3
323		300		
334	302			
378	324	370	336	Parallel x-translation, C_bH_3
470		480		Breathing, all $CH_{3,b}$
500				
569		565		
596			590	C_tH_3, rock
609		605		
631		650		Asymmetric breathing, all $CH_{3,t}$
682				Bending around Al–C bonds
		710		
762				CH_3 bending around Al–C bonds
1190				
1235			1233–1275	
1428			1427–1449	Symmetric CH_3 deformation
			2897–3003	CH stretch

intermolecular interaction. The CLIMAX program [16] is based on empirical assignment of characteristic bands based in our case on dimeric units. The assignment of internal modes is further guided by the GAUSSIAN94 *ab initio* calculation (see below). Furthermore, CLIMAX compares measured intensities with calculated mode structure factors. The bridging b-methyl group represents a weak link. Thus the dimer is strongly non-rigid and the most characteristic internal mode of the dimer (the bend around the C_b–C_b axis) appears in the regime of external modes at very low energies. Rotational potentials of terminal and bridging methyl groups become significantly different in the case of dimers due to the different bond characters. Three librational bands have to be assigned. Two bands showing strong isotope effects of librations are observed around 12 meV and at about 18 meV. The bands both show a multiplet structure due to the number of different eigenmodes of coupled rotors and due to dispersion. The band at lower energies is attributed to terminal CH_3 groups. From their large tunnel splittings and from the activation energy of the broadening and shift, respectively, with temperature, a band is expected in this regime of energies. Quasielastic spectra further confirm the assignment (see below). Similarly, the high-energy band is attributed to the bridging CH_3 groups.

2.4. Classical reorientational motion

With increasing temperature, methyl groups start to reorient classically by means of jumps over the rotational barrier. This process leads to quasielastic scattering and is represented by a δ-function whose Q-dependence is the elastic incoherent structure factor and a Lorentzian $L(\Gamma, \omega)$. The presence of N inequivalent methyl groups leads to a superposition of Lorentzians:

$$S(Q, \omega) = (1 - 2j_0)\delta(\omega) + \sum_{n=1}^{N} p_n(2 - 2j_0)L(\Gamma_n, \omega) \tag{3}$$

with

$$\sum_{n=1}^{N} p_n = 1.$$

The linewidths Γ_n of the Lorentzians are determined by the average time τ_n between two jumps, $\Gamma_n = 3/(2\tau_n)$, which follow Arrhenius laws:

$$\tau_n = \tau_0 \exp\left(-\frac{E_a^{(n)}}{kT}\right).$$

If one can decompose the quasielastic scattering into its n components, a measurement of the temperature-dependent linewidths yields the activation energies $E_a^{(n)}$ of all inequivalent methyl groups. E_a is generally assumed to represent the distance between the librational ground state and the top of the rotational potential [12].

Quasielastic neutron spectra were measured at the cold multichopper time-of-flight spectrometer NEAT of the HMI, Berlin, Germany, in the temperature regime $10 < T$ (K) < 234. At a wavelength $\lambda = 7$ Å the energy resolution of $\delta E_{res} = 52$ μeV is obtained. The spectra are shown in figure 3 and represent sums over 70 detectors in the angular range $80 < 2\Theta$ (deg) < 136.

Fitting a number of quasielastic Lorentzians into these overlapping sublines requires one to impose restrictions on the parameters. Otherwise the parameters become strongly correlated. From diffraction studies, we know [10] of the existence of $N = 3$ components with intensity ratios 1:1:1. The equal occurrence probability of the two terminal methyl groups is further confirmed by the tunnelling spectrum at low temperature (figure 1). Due to different barrier heights, the different lines enter the energy window of the spectrometer successively with increasing temperature.

A problem arises due to the phonon spectrum, which becomes more pronounced with increasing temperature. The simplest way to overcome this is to exclude the regime of large energy gain transfers from the fit. A more complete description has to include a phonon density of states (DOS) in the fit, measured at very low temperature, where it is not contaminated by quasielastic scattering. This requires one to measure the DOS without a quasielastic contribution. In view of the low rotational barriers present in $Al_2(CH_3)_6$, such a measurement would have to be performed at very low temperature, e.g. $T \sim 20$ K. The corresponding weak phonon DOS has to be thereafter transformed to higher temperatures by applying a Bose factor. It thus would become very noisy and lead to deterioration in the data analysis results. Thus, for the moment we used the first method, limiting the fitting range to energy transfers above -2 meV. Figure 4 shows an Arrhenius plot for the three components. While the strong potential of the bridging CH_3 group appears in a well separated temperature regime, the rather similar barriers of the terminal groups can be distinguished at low temperatures only, where the relative difference of their widths is largest. At these temperatures, $T \leqslant 90$ K, the quality of the fit, χ^2, is significantly improved by the use of two Lorentzians. The overall quasielastic

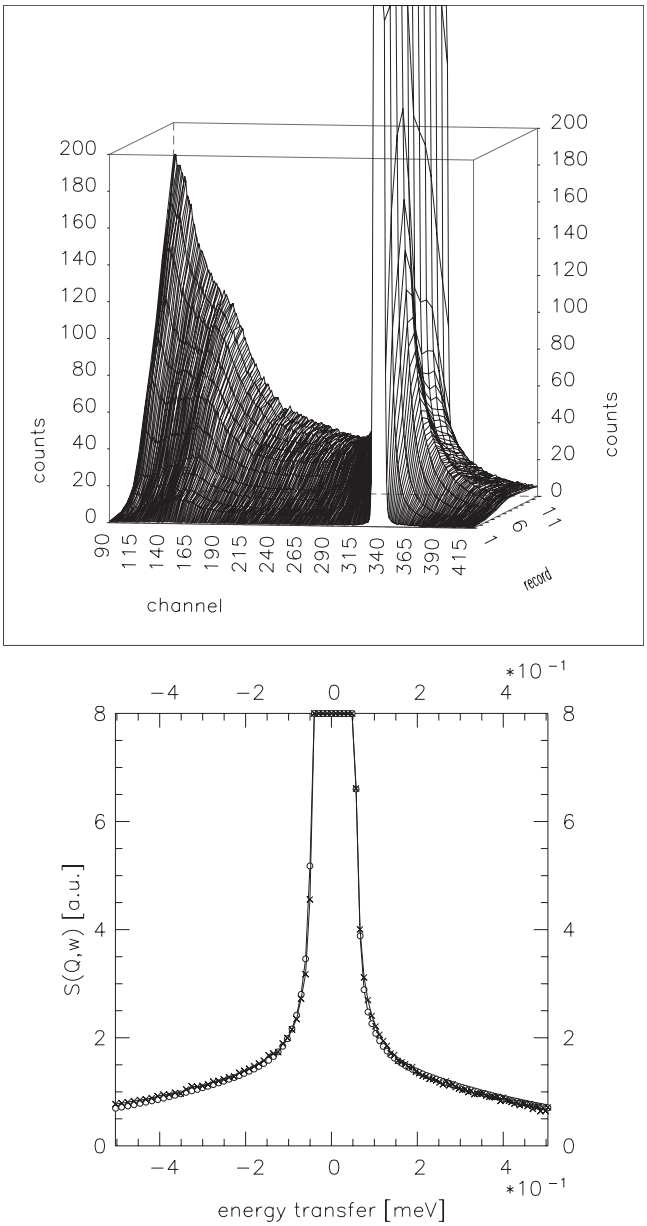

Figure 3. Top: some quasielastic spectra (counts versus channel) of $Al(CH_3)_3$. The axis 'record' corresponds to increasing temperature. Each spectrum represents the sum over 16 detectors. Bottom: the sum over 70 detectors each in the angular range $80 < 2\Theta$ (deg) < 136. Sample temperature $T = 139$ K. The solid curve with open circles is a fit with three Lorentzian of equal weight. Elastic peak intensity: 320. Instrument: NEAT at HMI, Berlin, Germany. $\lambda = 7$ Å.

intensities diminish at the highest temperature, $T = 234$ K, like that of the elastic line, by almost a factor 2. This is due to the strong Debye–Waller factor related to the weakly bonded dimeric unit. The fitted linewidths clearly follow exponential laws. The activation energies extracted are $E_a = 14.5$, 17.6 and 53.6 meV. The prefactors of the Arrhenius laws obtained

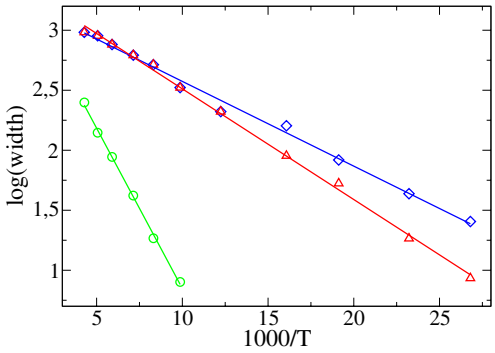

Figure 4. Arrhenius plots of the three components contained in the quasielastic spectra. Instrument: NEAT at HMI, Berlin.

Table 3. The rotational potentials (columns 4–6) are derived from $\hbar\omega_t$ and E_a. The librational modes E_{01} calculated are shown in the last column as a basis for discussing assignments in the DOS. Excitations shown in brackets are calculated in the single-particle model.

Isotope	$\hbar\omega_t$ (μeV)	E_a (kJ mol^{-1})	k	V_3 (meV)	V_6 (meV)	E_{01} (meV)
H	(0.33)	5.17		63	—	17.6
H	12.63	1.70	0	25.0	5.5	12.4
H	16.24	1.40	0	20.7	9.7	12.7
D	—	(5.44)		63	—	12.8
D	(0.24)	(1.88)	0	25.0	5.5	9.8
D	(0.31)	(1.62)	0	20.7	9.7	10.6

are rather similar and represent an attempt frequency. Their numerical values of about 4 meV are characteristic of rotating methyl groups.

They differ only weakly in the many systems studied so far. The assignment to tunnelling transitions is done such that the largest tunnel splitting is related to the lowest barrier (table 3). In this way, a misassignment is possible only for the terminal CH_3.

2.5. Ab initio calculations (GAUSSIAN94)

We have performed our own density functional calculations on the CRAY T90 using the GAUSSIAN94 program with the B3-LYP functional. A 6-31G*(d) basis set is applied for all atoms. Energy minimization was performed until a gradient of less than 3×10^{-4} Hartree Bohr^{-1} was obtained. A following vibrational analysis yielded eigenenergies and eigenvectors. Both the frequencies and the mode characters are shown in table 2. Internal modes coincide reasonably well with measured IR energies [4]. Calculated methyl librations and deformations of the whole molecule appear at rather low energies and may provide a test of the precision of the calculation.

Since the GAUSSIAN94 calculation deals with a single dimer, collective lattice modes like acoustic phonons cannot be reproduced. Corresponding bands have to be added intentionally.

The internal barrier of the bridging CH_3 was calculated in a type of single-particle model. The group was rotated by angular increments around its symmetry axis. The angle-dependent part of the total energy of the dimer was identified with the rotational potential. Two approaches were used. At first the molecule was fixed in its equilibrium orientation while the bridging

CH_3 group was rotated. This led to a too strong potential. Adiabatic rotation on the other hand allows the molecule to find its minimum-energy configuration at any orientation of the bridging CH_3 group. The rotational potential obtained in this way is weaker, but still stronger than found in the experiment. Our results cannot confirm an earlier *ab initio* calculation [17] which has found a rotational barrier of 20 kcal mol^{-1}.

3. Discussion

3.1. Methyl rotational potentials

We have identified in the present experiment three features for each species of methyl group characteristic of its rotational potential within the single-particle model: the tunnelling splitting, the librational mode and the activation energy. While the tunnel splitting and the activation energy have an unambiguous meaning, librational bands of a measured DOS may not match the single-particle description. For weak barriers, they fall into the regime of phonons and show dispersion like any lattice mode. Multiple eigenvectors in non-Bravais lattices lead to further band structure. These difficulties are especially clear for dimethylacetylene, where dispersion removes all intensity of the DOS from the nominal single-particle librational energy and creates three new bands at higher and lower energies. A consistent description became possible only recently [18] on the basis of a full structure analysis. For the reasons outlined, we use tunnel splittings and activation energies to determine the rotational potentials:

$$V(\varphi) = \sum_{n=1}^{2} \frac{V_{3n}}{2}(1 - (-1)^k \cos(3n\varphi)). \tag{4}$$

The assignment is done such that low tunnel splittings are connected with large barriers. Calculated methyl librational modes (table 3) are used to discuss peaks and isotope effects of the measured DOS.

The potential of the bridging methyl group can be refined only to first order due to the lack of information on tunnelling. However, the pure $\cos(3\varphi)$ potential accounts well for the measured librational band extending from 16 to 19 meV (figure 2). In the case of terminal methyl groups, an additional sixfold term of the order of 20–30% is found. Diffraction shows that protons of terminal CH_3 units are found in out-of-plane positions with respect to the plane of the four terminal carbon atoms. This plane is almost a mirror plane of the dimer and thus leads to the strong sixfold term of the rotational potential. The calculated librational bands from 12.4 and 12.8 meV correspond well with the measured librational DOS around 12–14 meV. A further confirmation of this assignment is given by the activation energies of the broadening of the tunnelling line at $\hbar\omega_t = 12.63$ μeV with temperature which reproduces very well the librational mode (table 1). The shift of the transition $\hbar\omega_t = 16.24$ μeV yields a somewhat lower value. This is in agreement with theory [12].

The activation energies obtained from quasielastic spectra of the protonated material can be compared with those from a NMR T_1-experiment [11]. The authors did not take into account inequivalency of methyl groups and thus obtained from the high-temperature slope of the spin–lattice relaxation only an average value $E_a = 3.5$ kJ mol^{-1}. Since E_a is based on an inappropriate model, it is of no real use.

3.2. Mode assignment and molecular structure

A satisfactory interpretation of TOSCA data in the high-energy regime was only possible assuming a dimerized unit with two bridging methyl groups. It thus confirms the dimer as the building unit of the solid.

Figure 5. The minimum-energy configuration of $Al_2(CH_3)_6$. The arrows indicate a bend mode of the whole molecule, about the bridging methyl groups. This mode has the absolutely lowest energy.

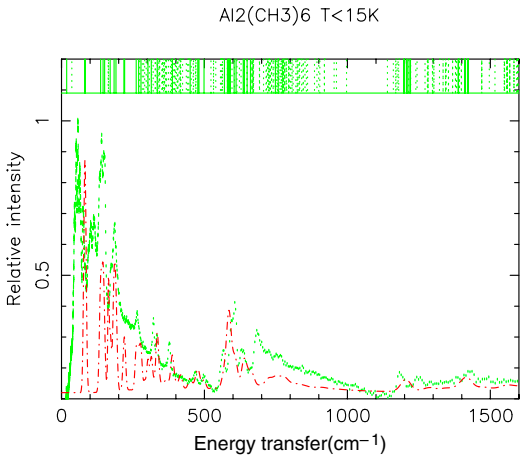

Figure 6. The fit (dot–dashed curve) of the protonated spectrum (error bars) using the CLIMAX program. Instrument: TOSCA at the ISIS Facility, RAL, UK. Sample temperature $T \sim 13$ K.

The methyl torsional modes were experimentally identified by the strongest isotopic shift and the coupling of quantum rotors to phonons [12]. These values are arranged in table 2 such that similar eigenmodes are found in the same line. The mode character is obtained from the GAUSSIAN94 calculation. Peaks in the neutron spectra (figure 6) fit well with these eigenenergies. The CLIMAX program links theory and experiment by evaluating neutron scattering structure factors.

The lowest-energy torsion at 5–8 meV is a collective motion of all four terminal CH_3 units with the eigenvector of a butterfly mode (figure 5). The mode is split into a multiplet by intermolecular coupling and due to the presence of $Z = 2$ dimers in the unit cell. This is surprising and exciting at the same time, since calculated data may deviate, especially for low-energy modes where the highest computational accuracy is required.

Differences between experimental results and *ab initio* calculations are expected, obviously, due to the absence of intermolecular interactions and periodicity.

The energy of the bridging methyl torsion is lower than calculated but significantly larger than the torsion of terminal methyl groups. At first glance this seems to be astonishing. An increased bond length, such as that found for Al–C_b, due to electron deficiency, usually leads to weaker rotational barriers [2]. However, in the present example the missing electron density

is used for a second weak bond to a second monomer. In the new dimer the bridging methyl group has lost its unique rotation axis. Rotation is connected with breaking and reconstructing two weak covalent C_b–Al bonds. This effect of internal steric hindrance massively overcompensates the weakening of the individual bond. Since the effect is intramolecular, the high barrier is reproduced in the *ab initio* calculation of the isolated molecule. At the same time it fits well with the barrier height obtained from quasielastic scattering.

3.3. Isotope effect

By means of neutrons, the isotope effect can only be observed for lattice and internal modes. The tunnelling lines are scaled down in energy such that they cannot longer be resolved. To get reliable potentials we keep the potential shape unchanged and rescale it by the lower rotational constant. This leads to librational energies in reasonable agreement with bands showing the strongest isotopic shift in the measured DOS (table 3).

4. Conclusions

Trimethylaluminium has recently attracted new interest. Firstly, this is due to its technical importance as an ingot for doping semiconductors with aluminium. Secondly, trimethylaluminium is the prototype of an electron deficiency compound involving methyl groups. Neutron spectroscopy can significantly contribute to a deeper understanding. Eigenmodes from the highest energies down to very low-energy vibrations can be explained mainly as modes of the soft symmetric dimer which is the building unit of the solid. It is found that methyl rotational potentials are best deduced from the tunnel splittings and activation energies extracted from quasielastic spectra. Librational modes calculated for these potentials fit well with those strong bands of the DOS which experience a strong isotope effect with deuteration. Methyl rotation is found to mirror the molecular structure. The loss of the σ-bond between aluminium and the bridging carbon with dimerization is accompanied with a pentacoordination of the carbon. This leads to a strong increase of its rotational potential compared to the only weakly affected terminal methyl groups. Since this potential is mainly of electronic origin (new bond symmetry), it is also well reproduced by the *ab initio* calculation of the isolated dimer. An overall good consistency of the phenomenological mode analysis with the *ab initio* calculations validates the corresponding data analysis code (CLIMAX).

Charge transfer between $M(CH_3)_3$ molecules leads to the formation of isolated dimers for M = Al, inequivalent monomers for M = Ga or weakly linked asymmetric tetramers for M = In. The varying connectivity between molecules makes this $M(CH_3)_3$ class of materials an interesting system in which to study delicately balanced intermolecular bonding.

Acknowledgments

We thank Dr H Hardtdegen of FZJ for supplying the protonated sample and Dr H Büttner of the ILL for the experimental confirmation that there are no other tunnelling transitions up to the free-rotor energy.

References

[1] Prager M and Heidemann A 1997 *Chem. Rev.* **97** 2933
[2] Müller-Warmuth W, Duprée k H and Prager M 1983 *Z. Naturf.* a **39** 66
[3] Downs A J (ed) 1993 *Chemistry of Aluminium, Gallium, Indium and Thallium* (London: Chapman and Hall)

[4] Koglin E, Koglin D, Meier R J and van Heel S 1998 *Chem. Phys. Lett.* **290** 99
[5] Almenningen A, Halvorsen S and Haaland A 1971 *Acta Chem. Scand.* **25** 1937
[6] Kvisle E and Rytter E 1984 *Spectrochim. Acta* A **40** 939
[7] Vranka R G and Amma E L 1967 *J. Am. Chem. Soc.* **89** 3121
[8] Lewis P H and Rundle R E 1953 *J. Chem. Phys.* **21** 986
[9] Huffman J C and Streib W E 1971 *Chem. Commun.* **1971** 911
[10] McGrady G S, Turner J F C, Ibberson R M and Prager M 2000 *Organometallics* **19** 4398
[11] Albert S and Ripmeester J A 1979 *J. Chem. Phys.* **70** 722
[12] Hewson A 1982 *J. Phys. C: Solid State Phys.* **15** 3841
Hewson A 1982 *J. Phys. C: Solid State Phys.* **15** 3855
[13] Frisch M J *et al* 1998 *Gaussian 98, Revision A.7* Gaussian Incorporated, Pittsburgh, PA
[14] Jullien J and Paillous A *Bull. Soc. Chim. Fr.* **1965** 2236
[15] Press W 1981 *Single Particle Rotations in Molecular Crystals (Springer Tracts in Modern Physics vol 81)* (Berlin: Springer)
[16] Kearley G, Tomkinson J and Champion D 2001 to be obtained from a-CLIMAX@rl.ac.uk
[17] Berthomieu D, Bacquet Y, Pedocchi L and Goursot A 1998 *J. Phys. Chem.* A **102** 7821
[18] Kirstein O, Prager M, Johnson M and Parker S F 2002 *Appl. Phys.* A at press